

CHEMICAL KINETICS
AND CATALYSIS

Gold-Doped Fe/TiO₂ Catalysts: A Case of Extra-Low Gold Loading in Glycerol Oxidation¹

E. A. Redina^{a,*}, K. V. Vikanova^a, A. A. Shesterkina^a, and L. M. Kustov^a

^aZelinsky Institute of Organic Chemistry, Russian Academy of Sciences, Moscow, Russia

* e-mail: redinalena@yandex.ru

Received December 22, 2017

Abstract—Au/Fe/TiO₂ catalysts with a low Au content (<0.1 wt %) were applied for the first time in liquid phase glycerol oxidation. A strong synergetic effect between Au and Fe cationic species was observed. The sample with an extra-low gold content (0.025 wt %) showed extremely high oxidation activity with TOF > 16000.

Keywords: gold-iron bimetallic catalyst, low-loading gold catalyst, oxidation, glycerol

DOI: 10.1134/S003602441811033X

INTRODUCTION

The oxidation of alcohols with oxygen is one of the most important transformations in modern organic chemistry, which can be used as a “green” atom-efficient approach to the synthesis of carbonyl and carboxy compounds [1, 2]. The oxidation of bio-derived alcohols is of a special interest. Among such alcohols one should consider glycerol. It is a cheap platform molecule obtained as a side product in bio-diesel production [3]. The benefit of glycerol oxidation is a broad scope of possible products with added value: aldehydes, ketones, and carboxylic acids [4].

Gold in a nanoparticle form has been recognized as an efficient catalyst for oxidation of various alcohols [5]. In the recent years, there is a trend in combining gold with other metals to obtain bimetallic structures with improved characteristics for selective oxidation catalysis [6, 7]. Thus, carbon supported Au–Pd bimetallic nanoparticles were successfully applied in glycerol oxidation to glyceric acid [8] or dihydroxyacetone [9]. An Au–Pt combination allows obtaining lactic acid [10, 11] and glyceric acid [12] from glycerol. Meanwhile, there are less examples of catalysts containing gold and non-precious metals used in alcohol oxidation reactions. Au–Cu NPs supported on mesoporous CeO₂–ZrO₂ showed high activity in selective glycerol oxidation to glyceric acid in water [13]. Unsupported Au–Cu NPs were used in liquid-phase 1,2-propanediol oxidation [14].

It should be noted that combination of gold in very small amounts (<0.2%) with base metals is a prominent way to obtain new bimetallic structures

with unique features in oxidation catalysis [15]. Recently we showed, that the low-loaded 0.2% Au/0.2% Cu/SiO₂ catalyst allowed selective ethanol oxidation to acetaldehyde with almost quantitative yield in gas phase [16]. Unfortunately, only a few works have been devoted to study the low-loaded gold catalysts [17–19], despite the fact that in the very first work on gold catalysis Bond et al. had already demonstrated the unusually high activity of 0.01% Au/SiO₂ in olefin hydrogenation [20]. Even less researches concerned the low-loaded “gold-base metal” bimetallic systems. Thus, the sample 0.1% Au–Bi/Al₂O₃ [21] and 0.25% Au–Cu/AC catalyst [22] were efficiently used in acetylene hydrochlorination reaction.

Herein we report on the first study of low-loaded Au/Fe/TiO₂ catalysts with improved activity in liquid-phase glycerol oxidation.

EXPERIMENTAL

The monometallic Fe/TiO₂ catalyst was prepared by deposition–precipitation with the urea (DPU) method. To obtain 1 g of the catalyst, a TiO₂ support (1 g, P 25, Acros Organics) was dispersed in DI water (30 mL). The suspension was stirred upon heating. When the temperature of the suspension reached 60°C, an aqueous solution of Fe(NO₃)₃ (0.4 mL, 0.45 M) was added to obtain the final Fe loading of 1 wt %. After that, the suspension was heated to 80°C under vigorous stirring and urea (1430 mg, Acros Organics) was added. The heating of the suspension was continued until the temperature reached 92°C, and the suspension was kept at this temperature under stirring for 4 h. Then the suspension was cooled down

¹ The article is published in the original.

to room temperature (RT), and the solid was isolated by centrifugation. The parent solution was checked for the presence of Fe^{3+} ions by adding KSCN to an aliquot amount of the parent solution. The test showed complete Fe deposition on the support. The solid was then washed three times with DI water (30 mL), dried under a vacuum at 40°C , and calcined at 400°C for 4 h. The catalyst was marked as 1Fe/TiO₂.

The monometallic parent catalyst was then modified with gold by a redox reaction [16]. The 1Fe/TiO₂ catalyst was first reduced in an H₂ flow (10 mL/min) at 450°C for 4 h in a U-shaped quartz reactor. After that, the reactor was cooled down to RT and a proper amount of an aqueous HAuCl₄ solution (1.2 mM) was added to obtain the gold loading equal to 0.5, 0.1, or 0.025 wt %. The obtained suspension was kept for 2 h, and then the solid was separated by centrifugation. The parent solution was checked for the presence of Au³⁺ ions by reverse iodometric titration [16], and the test showed complete gold deposition on the parent catalyst 1Fe/TiO₂. The solid was then washed with DI water (three times with 30 mL of DI water) and dried at 40°C under a vacuum.

The morphology of the samples was studied by scanning electron microscopy (SEM) and transmission electron microscopy (TEM). A target-oriented approach was utilized for the optimization of the analytic measurements [23]. Before SEM measurements the samples were mounted on a 25 mm aluminum specimen stub, fixed by conductive carbon paint and coated with a thin film (15 nm) of carbon. The observations were carried out using a Hitachi SU8000 field-emission scanning electron microscope (FE-SEM). Images were acquired in a secondary electron mode at the 2 kV accelerating voltage and at the working distance 4–5 mm. Morphology of the samples was studied taking into account a possible influence of carbon coating on the surface. To obtain TEM images, before measurements the samples were deposited on 3 mm carbon-coated copper grids from an isopropanol suspension. Samples morphology was studied using a Hitachi HT7700 transmission electron microscope. Images were acquired in a bright-field TEM mode at the 100 kV accelerating voltage.

DRIFT spectra were recorded using a Nicolet Protégé 460 spectrometer in the interval of 6000–400 cm⁻¹ at a resolution of 4 cm⁻¹ (500 scans). The adsorption of CO was performed at RT and a CO equilibrium pressure of 20 Torr. Before the experiments, the monometallic samples were treated at 400°C in a vacuum for 2 h. The bimetallic samples were evacuated for 2 h at 90°C .

Diffuse-reflectance spectra in the UV–Vis range (200–850 nm, UV–Vis DRS) were recorded with a Hitachi M-340 spectrometer supplied with an integrating sphere attachment using a MgO pellet as a ref-

erence. The spectra were recorded for powdered TiO₂ and the 1Fe/TiO₂ catalyst placed in a quartz chamber.

The oxidation of glycerol was performed in a liquid phase in a lab-constructed finger-type autoclave (inner volume 10 mL) at 90°C and an O₂ pressure of 5 bar. In the experiment, the weighed amount of the catalyst (11 mg) was placed in the inner glass insert and then an aqueous solution of glycerol (0.5 mL, 0.3 M) was added to the catalyst. The reaction was performed in water under alkaline conditions with NaOH to glycerol ratio 1.7. The glass inner part was inserted in the autoclave. The reactor was closed, flushed with nitrogen and O₂ for 3 times. After adjusting O₂ pressure (5 bar), the reactor was placed on an oil bath heated to the desired temperature. The reaction was carried out for 2 h under stirring at 800 rpm at 90°C . After that, the reactor was cooled down to RT. The catalyst was isolated by centrifugation and the clear solution of the reaction products was collected.

The analysis of the products was performed using NMR spectroscopy. ¹H Spectra of the reaction mixture were recorded on a Bruker AV300 spectrometer using a mixture of H₂O and D₂O (from 75 to 25%) as a solvent and benzoic acid as an external standard. The presaturation technique was used to suppress the water signal; yields and molar ratios of the products were calculated by integration of the signals in ¹H NMR spectra on the basis of 3H. Assignments of proton signals: ¹H NMR (300 MHz, H₂O + D₂O) glycerol: δ 3.45–3.67 (4H, m, CH₂(OH)), 3.70–3.80 (1H, m, CH(OH)); lactic acid: δ 1.31 (3 H, d, $J = 6.9$ Hz, CH₃), 4.09 (1H, q, $J = 6.9$ Hz, CH(OH)); acetic acid: δ 1.90 (3 H, s, CH₃); glyceric acid: δ 3.65–3.83 (2 H, m, CH₂(OH)), 4.05–4.07 (1H, m, CHOH), glycolic acid: δ 3.92 (2 H, s, CH₂(OH)); tartronic acid: δ 4.32 (1H, s, CH(OH)); formic acid: δ 8.42 (1H, s, CH(O)OH).

RESULTS AND DISCUSSION

The DRIFT-CO spectrum of the monometallic 1Fe/TiO₂ (Fig. 1, curve *a*) catalyst reveals the presence of Fe³⁺ cations as a band observed at 2362 cm⁻¹ that can be assigned to Fe²⁺–CO₂ complexes formed by oxidation of CO with Fe₂O₃ [24, 25]. The intense band at 2177 cm⁻¹ is attributed to Ti⁴⁺–CO linear carbonyl [24, 25]. The UV–Vis spectra of 1Fe/TiO₂ and TiO₂ are presented in Fig. 2. The subtraction of the TiO₂ spectrum from the 1Fe/TiO₂ spectrum gives the final spectrum with a maximum at 398 nm and a shoulder at 478 nm (Fig. 2). The band at 398 nm can be attributed to octahedral Fe³⁺ in small oligomeric Fe_xO_y clusters, while the band at 478 nm presumably corresponds to bulk Fe₂O₃ oxide [26, 27].

After redox deposition of the extra-low amount of gold (0.025 wt %) onto 1Fe/TiO₂, the band attributed

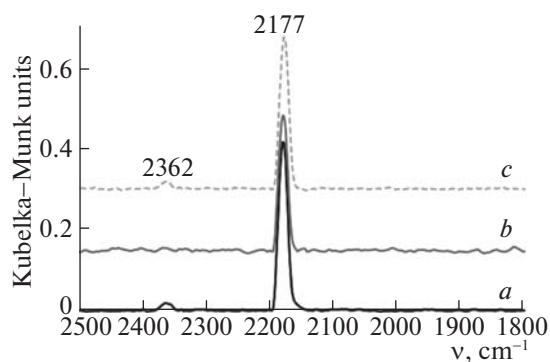


Fig. 1. DRIFT-CO spectra of 1Fe/TiO₂ (a), 0.025Au/1Fe/TiO₂ (b), and 0.5Au/1Fe/TiO₂ (c) at 20°C and 14 Torr of CO.

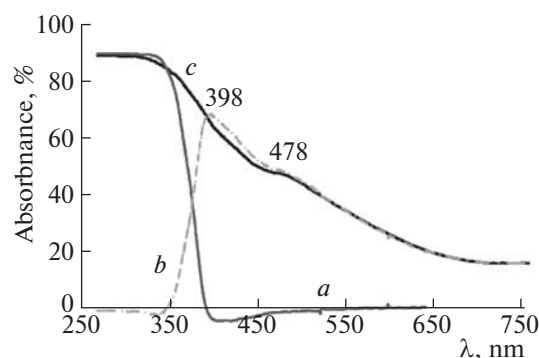


Fig. 2. UV-Vis DR spectra of TiO₂ (a), 1Fe/TiO₂ (b), and resulting spectra obtained after subtraction of the TiO₂ spectrum from the spectrum of 1Fe/TiO₂ (c).

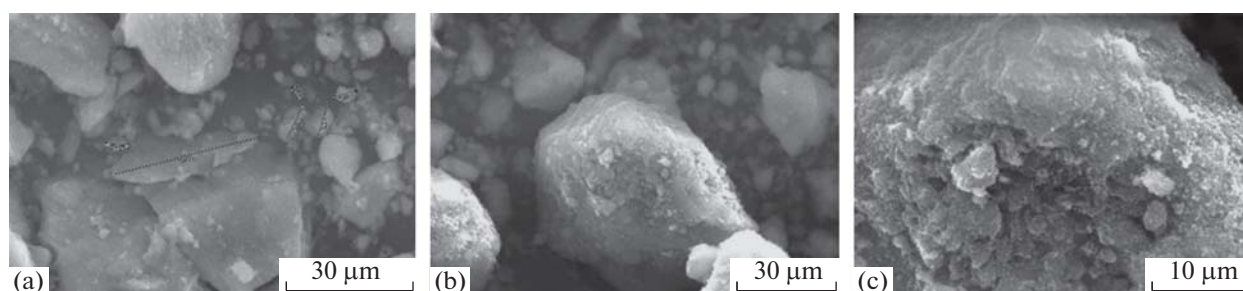
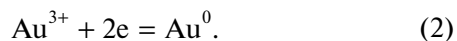


Fig. 3. SEM images of 1Fe/TiO₂ (a) and 0.5Au/1Fe/TiO₂ (b, c).

to Fe²⁺-CO₂ disappeared from the DRIFT spectra of adsorbed CO indicating the reduction of Fe³⁺ species during H₂ treatment of the catalyst before Au deposition (Fig. 1, curve b). However, in the spectra of 0.5Au/1Fe/TiO₂ there is a band of Fe²⁺-CO₂ at 2362 cm⁻¹ (Fig. 1, curve c). This can be explained by reoxidation of the surface Fe²⁺ cations (reduced under H₂ thermal treatment) with Au³⁺ during the direct redox reaction according to the semi-reactions:



It should be noted that the bands of Fe²⁺-CO and Auⁿ⁺-CO may also exist in the spectra of bimetallic catalysts, but overlap with the Ti⁴⁺-CO band. Thus, the amount of Fe³⁺ in the 0.025Au/1Fe/TiO₂ catalyst is much lower than that in 0.5Au/1Fe/TiO₂.

The reduction of the monometallic catalyst with subsequent Au redox deposition completely changed the surface morphology of the catalysts (Fig. 3). The 1Fe/TiO₂ sample is characterized by a smooth surface (Fig. 3a), while the surface of the bimetallic 0.5Au/1Fe/TiO₂ catalyst is loose and rough (Figs. 3b, 3c).

The redox method applied to deposit gold on 1Fe/TiO₂ allowed the formation of small nanoparticles with an average size 3 nm. The size distribution of nanoparticles is close to uniform; large nanoparticles with the size 8–11 nm can be seen along with the small ones with the size 1–2 nm (Fig. 4).

The activity of the prepared bimetallic catalysts in glycerol oxidation strongly depends on the amount of gold deposited by the redox method.

The interaction of gold with iron oxide improved the activity of gold catalysts. Compared to the monometallic 0.5Au/TiO₂ system, the bimetallic sample 0.5Au/1Fe/TiO₂ showed a higher selectivity to carboxylic acids and increased conversion of glycerol (Table 1, entries 1, 3). The main products were glyceric, glycolic and oxalic acids. The TOF value of the bimetallic catalyst was higher than that of monometallic 0.5Au/TiO₂, while 1Fe/TiO₂ showed low activity under the conditions used. Thus, the strong synergetic effect was observed for the Au/Fe/TiO₂ bimetallic catalyst.

The most unusual results were obtained when the amount of gold in the bimetallic catalyst was reduced to the value as low as 0.025 wt %. The extremely high TOF >16000 was observed for the 0.025Au/1Fe/TiO₂ catalyst, and the glycerol conversion reached 30%.

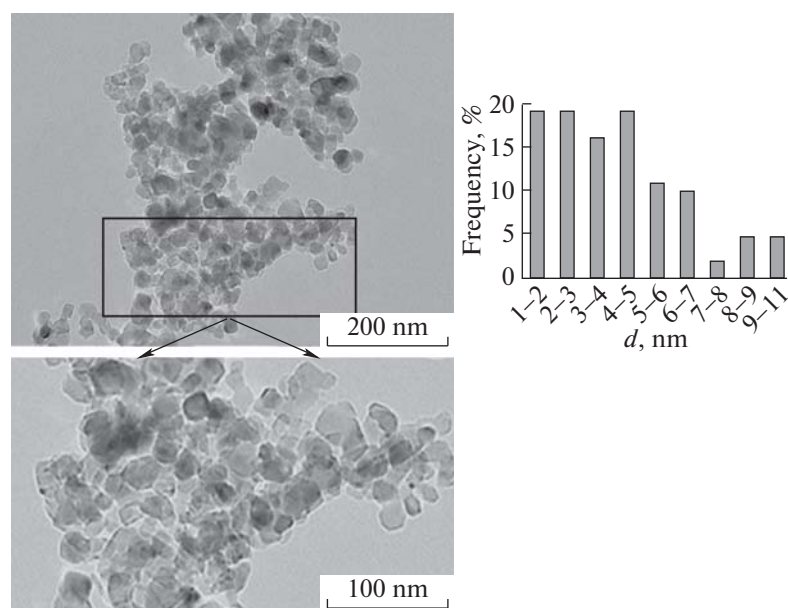


Fig. 4. TEM images of 0.5Au/1Fe/TiO₂ and the particle size distribution.

However, the oxidation activity of this sample was so high that glycerol oxidation proceeded mostly to CO₂ and the precision of carbon balance was only 78% (Table 1, entry 5). When the amount of gold was increased to 0.1%, the conversion of glycerol improved and reached 44%. The selectivity to carboxylic acids also became higher. TOF decreased compared to TOF of the 0.025Au/Fe/TiO₂ sample, but still was much higher than TOFs of the 0.5Au/TiO₂ and 0.5Au/1Fe/TiO₂ catalysts (Table 1, entry 4).

The high oxidation activity of low-loaded Au/Fe/TiO₂ catalysts can be due to the different state of Fe and Au in these samples compared to the 0.5Au/1Fe/TiO₂ catalyst. The DRIFTS-CO study of the low-loaded 0.025Au/1Fe/TiO₂ catalyst showed that the amount of Fe³⁺ in this sample is too low to be visible in the spectrum, while in the spectrum of

0.5Au/1Fe/TiO₂ the band of Fe³⁺ cations was clearly observed. During the oxidation reaction, Fe²⁺ cations in low-loaded bimetallic catalysts can be reoxidized to surface Fe³⁺ cations. We assume that combination of in-situ generated Fe³⁺ cations and gold is responsible for the oxidation activity of low-loaded bimetallic catalysts. In addition, gold deposited on the support in such small concentrations usually presents in a cationic form with induced oxidation activity, as it was observed in previous works [28, 29].

CONCLUSIONS

A strong synergetic effect between Au and iron oxide species in gold-doped Fe/TiO₂ catalysts prepared by the redox method was observed in the glycerol oxidation reaction. The oxidation activity of the catalysts is dependent on the amount of gold deposited

Table 1. The activity of the prepared catalysts in the glycerol oxidation reaction

Entry	Sample	TOF	X, %	C _{bal} , %	Selectivity, %					
					LA	AA	OA	GlyA	TA	GcA
1	0.5Au/TiO ₂	1155	43	69	2	0	2	19	0	3
2	1Fe/TiO ₂	—	11	91	0	0	2	3	0	5
3	0.5Au/1Fe/TiO ₂	1477	55	86	5	0	18	24	1	26
4	0.1Au/1Fe/TiO ₂	4063	44	79	8	0	15	2	0	28
5	0.025Au/1Fe/TiO ₂	16116	30	78	1	0	6	7	0	13

Reaction conditions: Aqueous glycerol solution (Gly) 0.3 M, 0.5 mL, NaOH : Gly 1.7, $m_{\text{cat}} = 11$ mg, $t = 90^\circ\text{C}$, $p(\text{O}_2) = 5$ bar, 2 h; TOF was calculated as mol (Gly)/[mol (Au) h⁻¹]. LA—lactic acid, AA—acetic acid, OA—oxalic acid, GlyA—glyceric acid, GcA—glycolic acid, X—conversion, C_{bal}—precision of carbon balance; the precision of carbon balance for all systems was not 100% because of complete glycerol oxidation to CO₂.

by the redox reaction, which, in turn, governs the oxidation state of gold and iron cationic species in the samples. The highest oxidation activity with TOF reaching 16 000 was observed for low-loaded Au/Fe samples with the Au content 0.025 wt %.

ACKNOWLEDGMENTS

The reported study was funded by RFBR according to the research project no. 16-33-00032. Electron microscopy characterization were performed by Dr. A. Kashin in the Department of Structural Studies of Zelinsky Institute of Organic Chemistry, Moscow. Authors thank Dr. O. Tkachenko for DRIFTS-CO study of the catalysts.

REFERENCES

1. Y.-F. Liang and N. Jiao, *Accounts Chem. Res.* **50**, 1640 (2017).
2. R. Ciriminna, V. Parus, F. Beland, et al., *Org. Process Res. Dev.* **19**, 1554 (2015).
3. A. Villa, N. Dimitratos, C. Chan-Thaw, et al., *Accounts Chem. Res.* **48**, 1403 (2015).
4. J. C. Beltran-Prieto, K. Kolomaznik, and J. Pecha, *Aust. J. Chem.* **66**, 511 (2013).
5. B. Chowdhury, C. Santra, S. Mandal, and R. Kumar, in *Advanced Materials for Agriculture, Food, and Environmental Safety*, Ed. by A. Tiwari and M. Syväjärvi (Wiley, Chichester, 2014), p. 197. doi 10.1002/9781118773857.ch8
6. G. J. Hutchings, *Catal. Today* **238**, 69 (2014).
7. C. Louis, *Catalysts* **6**, 110/1 (2016)
8. A. A. Rodriguez, C. T. Williams, and J. R. Monnier, *Appl. Catal., A* **475**, 161 (2014).
9. S. Hirasawa, H. Watanabe, T. Kizuka, et al., *J. Catal.* **300**, 205 (2013).
10. R. K. P. Purushothaman, J. van Haveren, D. S. van Es, et al., *J. Appl. Catal., B* **147**, 92 (2014).
11. E. A. Redina, O. A. Kirichenko, A. A. Greish, et al., *Catal. Today* **246**, 216 (2015).
12. C. Xu, Y. Du, C. Li, et al., *Appl. Catal., B* **164**, 334 (2015).
13. P. Kaminski, M. Ziolek, and J. A. van Bokhoven, *RSC Adv.* **7**, 7801 (2017).
14. W. Xue, H. Yin, Z. Lu, et al., *Catal. Lett.* **146**, 1139 (2016).
15. V. P. Ananikov, K. I. Galkin, M. P. Egorov, et al., *Mendeleev Commun.* **26**, 365 (2016).
16. E. A. Redina, A. A. Greish, I. V. Mishin, et al., *Catal. Today* **241**, 246 (2015).
17. A. Murugadoss, K. Okumura, and H. Sakurai, *J. Phys. Chem. C* **116**, 26776 (2012).
18. E. Redina, A. Greish, R. Novikov, et al., *Appl. Catal. A* **491**, 170 (2015).
19. E. A. Redina, O. A. Kirichenko, A. A. Greish, et al., *Catal. Today* **246**, 216 (2015).
20. G. C. Bond and P. A. Sermon, *Gold Bull.* **6**, 102 (1973).
21. J. Zhao, X. Cheng, L. Wang, et al., *Catal. Lett.* **144**, 2191 (2014).
22. J. Zhao, S. Gu, X. Xu, et al., *RSC Adv.* **5**, 101427 (2015).
23. V. V. Kachala, L. L. Khemchyan, and A. S. Kashin, *Russ. Chem. Rev.* **82**, 648 (2013).
24. A. A. Davydov, *Molecular Spectroscopy of Oxide Catalyst Surfaces* (Wiley Interscience, New York, 2003), p. 466.
25. K. I. Hadjiivanov and G. N. Vayssilov, *Adv. Catal.* **47**, 307 (2002).
26. M. S. Kumar, M. Schwidder, and W. Grunert, *J. Catal.* **227**, 384 (2004).
27. S. Pradha and B. Mishra, *RSC Adv.* **5**, 86179 (2015).
28. A. M. Visco, F. Neri, G. Neri, et al., *Phys. Chem. Chem. Phys.* **1**, 2869 (1999).
29. R. M. Finch, N. A. Hodge, G. J. Hutchings, et al., *Phys. Chem. Chem. Phys.* **1**, 485 (1999).